STK38 kinase acts as XPO1 gatekeeper regulating the nuclear export of autophagy proteins and other cargoes

Alexandre PJ Martin[1,2], Maarten Jacquemyn[3], Joanna Lipecka[4,5], Cerina Chhuon[5,6], Vasily N. Aushev[7], Brigitte Meunier[1,2], Manish K Singh[1,2], Nicolas Carpi[2,8], Matthieu Piel[2,8], Patrice Codogno[5,9], Alexander Hergovich[10], Maria Carla Parrini[1,2], Gerard Zalcman[1,2,11], Ida Chiara Guerrera[5,6], Dirk Daelemans[3], Jacques H Camonis[1,2]

[1] ART group, Inserm U830

[2] Institut Curie, Centre de Recherche, Paris Sciences et Lettres Research University, 75005 Paris, France

[3] KU Leuven Department of Microbiology, Immunology and Transplantation. Laboratory of Virology and Chemotherapy, Rega Institute for Medical Research, KU Leuven, 3000 Leuven, Belgium

[4] Inserm U894, Center of Psychiatry and Neuroscience, Paris, France

[5] Université Paris Descartes, Sorbonne Paris Cité, Paris, France

[6] Proteomics platform 3P5-Necker, Université Paris Descartes - Structure Fédérative de Recherche Necker, INSERM US24/CNRS UMS3633, Paris 75014, France.

[7] Icahn School of Medicine at Mount Sinai, 1 Gustave Levy Place, New York, NY 10029, USA

[8] CNRS, UMR 144

[9] Inserm U1151/CNRS UMR 8253, Institut Necker Enfants-Malades

[10] University College London, Cancer Institute, London, WC1E 6BT, United Kingdom

[11] Université Paris Diderot, Sorbonne Paris Cité, Paris, France

Table of Contents:

Appendix Figures Legends

Appendix Figure S1 (in support of Figure 1). Validation of nutrient starvation-induced autophagy and biotinylation.

(**A**) Western Blots show protein level for both autophagic markers p62 and LC3 from cell lysates identical to the ones used for mass spectrometry identification.

(**B**) Graphical representations show a significant decrease of both autophagic markers p62 and LC3 upon EBSS incubation indicating a good autophagy induction (n = 3 independent experiment, Mann-Whitney test). *p<0.05; **p<0.01; ***p<0.001; ns, not significant. Graphs represent mean ± standard error of the mean (SEM).

(**C**) Western blot revealing biotinylation pattern of whole cell lysates identical to the ones used in mass spectrometry for the nutrient starvation-induced autophagy condition.

(**D**) Western blot revealing biotinylation pattern of whole cell lysates identical to the ones sent to mass spectrometry for the suspension condition.

(**E**) Correlation matrix of the three replicates for both nutrient starvation-induced autophagy and ECM detachment conditions based on the association fold of STK38 newly identified partners using Pearson correlation indicating good reproducibility between each replicate. Circles size and colour represent the correlation coefficient (blue for positive, red for negative).

Appendix Figure S2 (in support of Figure 2). Validation of XPO1 inhibition and autophagy monitoring cell line.

(**A**) Validation of XPO1 activity inhibition as shown in Figure 2. HeLa cells were incubated with DMEM or EBSS in the presence of XPO1 inhibitors KPT-185 or KPT-330 as indicated (final concentration = 1 µM) or DMSO for 4 hours. Cells were then fixed and stained for endogenous IκBα, a well known XPO1 cargo. Representative images are shown and scale bars are 40 µm.

(**B**) Graphical representation of IκBα nuclear staining/cytoplasmic staining (n > 30 cells from 3 independent experiments, Mann-Whitney test). As anticipated, XPO1 activity inhibition by KPT-185 or KPT-330 induced a nuclear retention of IκBα. *p<0.05; **p<0.01; ***p<0.001; ns, not significant. Graphs represent mean ± standard error of the mean (SEM).

(**C-D**) Validation of autophagy monitoring cell line.

(**C**) HeLa cells stably expressing the GFP-LC3-RFP-LC3ΔG reporter autophagic probe [1] were incubated with the indicated siRNA. 72h later, cells were incubated with DMEM or EBSS for 4 hours and the GFP and RFP signals were recorded by FACS analysis and then shown as a GFP-LC3/RFP-LC3ΔG ratio (%) (n=4 independent experiments, Mann-Whitney test). As expected, nutrient starvation incubation induced a significant decrease of the GFP-LC3/RFP-LC3ΔG ratio that is stopped when the pro autophagic proteins ATG5 and Beclin1 are silenced. As expected also, STK38 silencing inhibited the autophagic process. *p<0.05; **p<0.01; ***p<0.001; ns, not significant. Graphs represent mean ± standard error of the mean (SEM).

(**D**) Validation of silencing of proteins indicated in (**D**). Western blot indicates good silencing of STK38, ATG5 and Beclin1 proteins when associated with their respective siRNA (numbers indicate the average protein level normalized on GAPDH level for the 4 replicates).

Appendix Figure S3 (in support of Figure 3). Validation of STK38 replacement and p62 levels.

(**A**) HeLa cells stably expressing the GFP-LC3-RFP-LC3ΔG reporter autophagic probe were transiently transfected with siRNA targeting the 3'UTR region of endogenous STK38 (or with non-targeting siRNA (siNT)). The next day, cells were transiently transfected with the indicated STK38 mutants expressing plasmids. 24 hours after, cells were incubated with DMEM or EBSS for 4 hours and then subjected to lysis and western blotting analysis (here, only one replicate is presented). This indicates a good replacement of STK38 in all conditions.

(**B**) Western-Blot of quantifications shown in Figure 3D (here, only one replicate of the three is presented). The figure indicates a good replacement of STK38 in all conditions.

Appendix Figure S4 (in support of Figure 4 and Figure EV2). Detection of XPO1_S1055 phosphorylation by mass spectrometry.

Annotated fragmentation spectra for peptide 1053-1070. HekRasV12 cells were transiently transfected with both Flag-XPO1(wt) and myc-STK38(wt) plasmids. 24 hours later, cells were treated with Okadaic Acid for 1 hour (final concentration = 1 µM). Flag-XPO1 was then immunoprecipited following mass spectrometry analysis. The MS/MS spectra were obtained on two different mass spectrometers, the TIMS TOF PRO (above, mascot ion score 70, expect value = 3.6e-06 , and the Q exactive Plus (below, mascot ion score = 39, expect value = 0.00022). Phosphorylation on S1055 is well confirmed by both spectra (fragments containing the phosphorylation –or the neutral loss of 98 - are flagged with a red dot).

Appendix Figure S5 (in support of Figure 5 and Figure EV3). XPO1 mutants transfection validation & STK38 silencing.

(**A**) Same cells used as in Figure 5B&C were subjected to whole cell lysis and western blotting analysis (here, only one replicate of the three is presented). This figure indicates that cells used are well transfected for myc-STK38(wt) and for Flag-XPO1 variants plasmids. Exogenous signal for XPO1 in C528S_ΔCter is absent (compared to the others) because the targeted amino acid sequence of the anti-XPO1 antibody is included in the Cter region deleted in this construct.

(B) Same cells used as in Figure 5E and Figure EV3B were subjected to whole cell lysis and western blotting analysis (here, only one replicate of the two is presented where the numbers indicate the average STK38 protein level normalized on GAPDH level for the 2 replicates).

Appendix Figure S6 (in support of figure 6 and Figure EV4). Validation of STK38 silencing and Beclin1 antibody.

(**A**) STK38 silencing. Same cells as used in Figure 6A and Figure EV4A were subjected for whole cell lysis and western blotting analysis in order to confirm STK38 silencing (numbers indicate the average STK38 protein level normalized on GAPDH level for the 3 replicates of the experiment). Results indicate here an efficient silencing of endogenous STK38.

(**B**) Validation of anti Beclin1 antibody used in Figure 6 and Figure EV4. HeLa and HAP1 wt cells were subjected to IF using anti Beclin1 or IgG control antibodies. The IFs with IgG control were black, demonstrating the specificity of the anti Beclin1 antibody, scale bars are 40 µm.

(**C**) STK38 silencing. Same cells used in Figure 6C and Figure EV4C were subjected for whole cell lysis and western blotting analysis in order to confirm STK38 silencing (here, only one replicate of the two is presented).

Appendix Figure S7 (in support of Figure 7 and Figure EV5). Validation of STK38 silencing and YAP1 protein level.

(**A**) Same cells as used in Figure 7A and Figure EV5A were subjected for whole cell lysis and western blotting analysis in order to confirm STK38 silencing (numbers indicate STK38 protein level normalized on GAPDH level for the 3 replicates of the experiment). Results indicate here an efficient silencing of endogenous STK38.

(**B**) Same cells as used in Figure 7A and Figure EV5A were subjected for whole cell lysis and western blotting analysis in order to check for YAP1 global protein level (numbers indicate the average YAP1 protein level normalized on GAPDH level for the 3 replicates of the experiment). Blots indicate that YAP1 protein levels remain approximatively identical between each conditions, indicating that YAP1 nuclear exclusion observed in Figure 7A and Figure EV5A is due to nuclear/cytoplasmic shuttling and not to protein degradation.

(**C**) Same cells as used in Figure 7B and Figure EV5B were subjected for whole cell lysis and western blotting analysis in order to check for YAP1 global protein level (numbers indicate the average YAP1 protein level normalized on GAPDH level for the 3 replicates of the experiment). Blots indicate that YAP1 protein levels remain approximatively identical between each conditions, indicating that YAP1 nuclear exclusion observed in Figure 7B and Figure EV5B is due to nuclear/cytoplasmic shuttling and not to protein degradation.

(**D**) STK38 silencing. Same cells used in Figure 7C and Figure EV5C were subjected for whole cell lysis and western blotting analysis in order confirm STK38 silencing (here, only one replicate of the two is presented).

(**E-F**) STK38 is not required for YAP phosphorylation on S127 and LATS2 protein level.

(**E**) A548 cells were seeded at low vs high confluence with the indicated set of siRNA. 72 hours later, cells were lysed and subjected to western blotting using the indicated antibodies. Silencing LATS1/2 results in a loss of phosphorylated YAP on S127 where knock down of STK38 does not impact YAP1 phosphorylation on S127.

(**F**) The same cells samples used in (**E**) were analysed for LATS2 protein expression in parallel of a positive control (H1299 cell line). The results indicate that the absence of signal in (**E**) when using the anti-LATS2 antibody is not due to experimental issue but rather on very low LATS2 protein expression in A549 cells.

Appendix Figure S8. XPO1 blockage phenocopies STK38 silencing for proper centrosome distribution.

(**A-B**) XPO1 is required for centrosome distribution.

(**A**) HeLa cells stably expressing GFP-Centrin were cultured on glass-bottom 6 well plates for two days in order to each 50% confluency the day of the experiment. GFP signal was then recorded on live microscopy and centrosomes (centrin “spots”) were counted on Z-stacks images without differentiating unique separated centrioles in G1 phase from separated centrosomes (harbouring 2 centrioles each) in S/G2 phase. Representative images are shown and scale bars are 40 µm. White arrows indicate centrosomes.

(**B**) Graphical representation of cell population harbouring one, two, or no centrosomes. (n> 300 cells from 13 different fields from 3 experiments, Mann-Whitney test). Here, XPO1 blockage significally impaired proper centrosomal distribution. *p<0.05; **p<0.01; ***p<0.001; ns, not significant. Graphs represent mean ± standard error of the mean (SEM).

(**C-E**) STK38 is required for centrosome distribution.

(**C**) HeLa cells stably expressing GFP-Centrin were transiently transfected with the indicated siRNA for two days. GFP signal was then recorded on live microscopy and centrosomes (centrin “spots”) were counted on Z-stacks images as described above. Representative images are shown and scale bars are 40 µm. White arrows indicate centrosomes.

(**D**) Graphical representation of cell population harbouring one, two, or no centrosomes. (n> 200 cells from 15 different fields from 3 experiments, Mann-Whitney test). Here, STK38 silencing significally impaired proper centrosome distribution. **p*<0.05; ***p*<0.01; ****p*<0.001; ns, not significant. Graphs represent mean ± standard error of the mean (SEM).

(**E**) STK38 protein level of cells shown in **C**, numbers indicate the average STK38 protein level normalized on GAPDH level for the 3 replicates of the experiment. Results indicate here an efficient silencing of endogenous STK38.

Appendix Figure S9. Diagram of the mechanism of activation of XPO1 by STK38.

Activated STK38 (triggered by T444 phosphorylation) phosphorylates inactivated XPO1 on S1055 within the auto-inhibitory domain (AI) resulting in a change of conformation of XPO1 and exposing its cargo binding region (NES, for Nuclear Export Signal recognition domain). Supposedly, the binding of Ran-GTP to its association domain (RAN) finalizes this process leading to the nuclear export of the cargo.

Appendix Figure S10. STK38 phosphorylation motif in XPO1 is conserved in simians.

XPO1 protein sequences among different systematic groups were aligned (only the C-terminal domain is shown). Amino acids highly conserved among all species are marked with blue color, less conserved are marked with pink color where non conserved are marked without color. Simians are highlighted in red and non-simian primates are highlighted in green. Red frame denotes location of the STK38 phosphorylation motif HxRxxS/T.

References

1. Kaizuka T, Morishita H, Hama Y, Tsukamoto S, Matsui T, Toyota Y, Kodama A, Ishihara T, Mizushima T, Mizushima N (2016) An Autophagic Flux Probe that Releases an Internal Control. *Mol Cell* **64**: 835–849.

Martin et al. - Appendix Fig S1

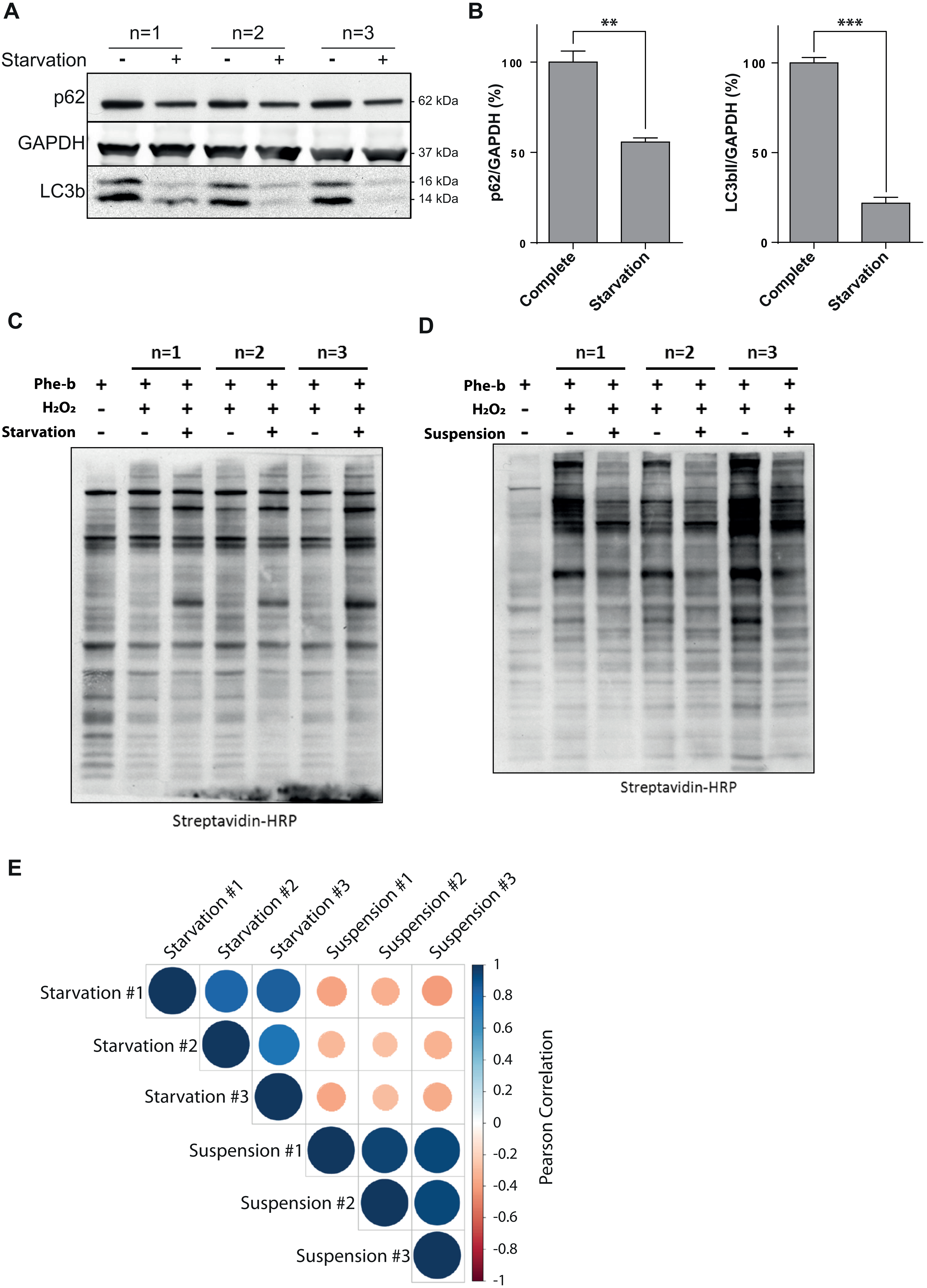

Martin et al. - Appendix Fig S2

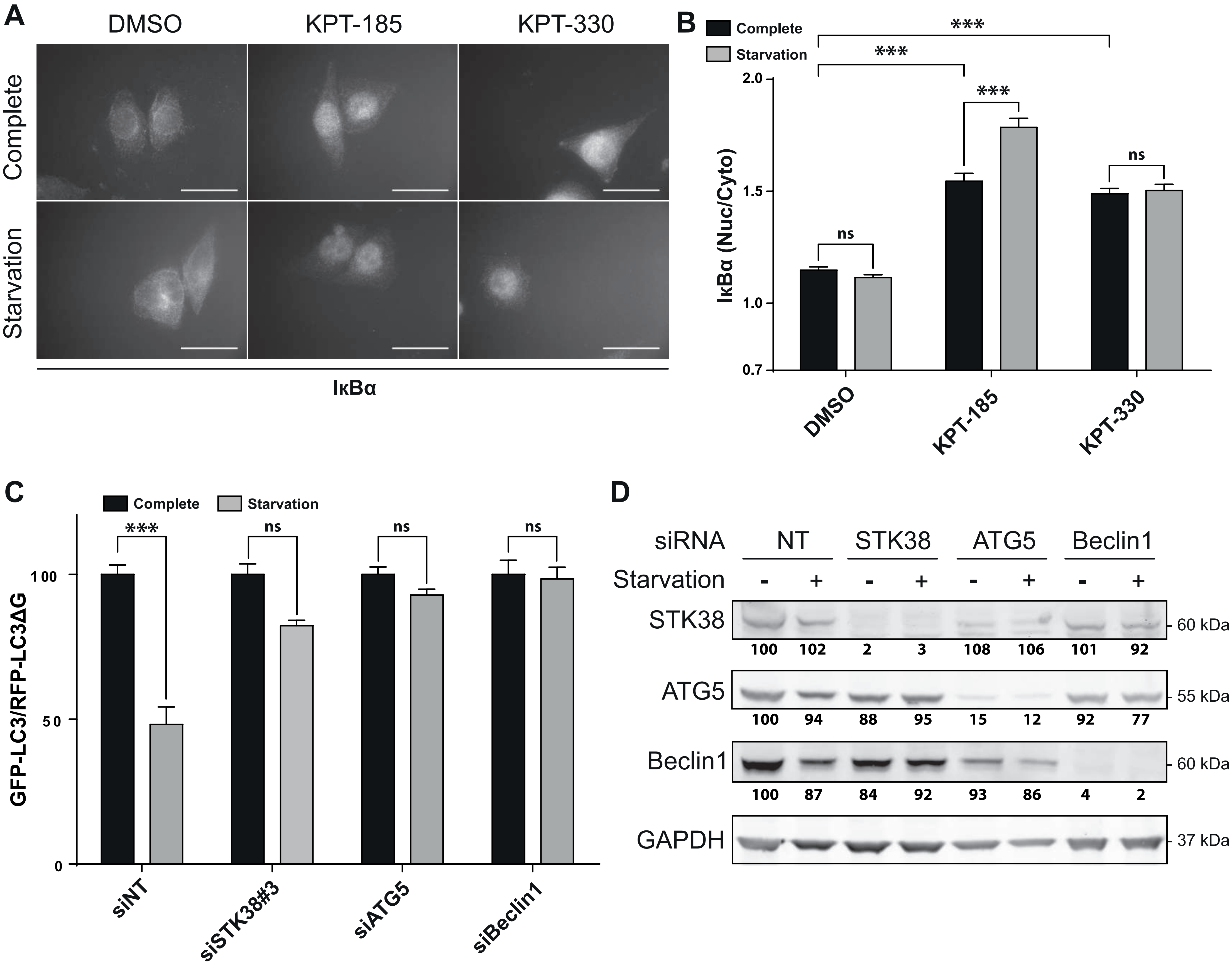

Martin et al. - Appendix Fig S3

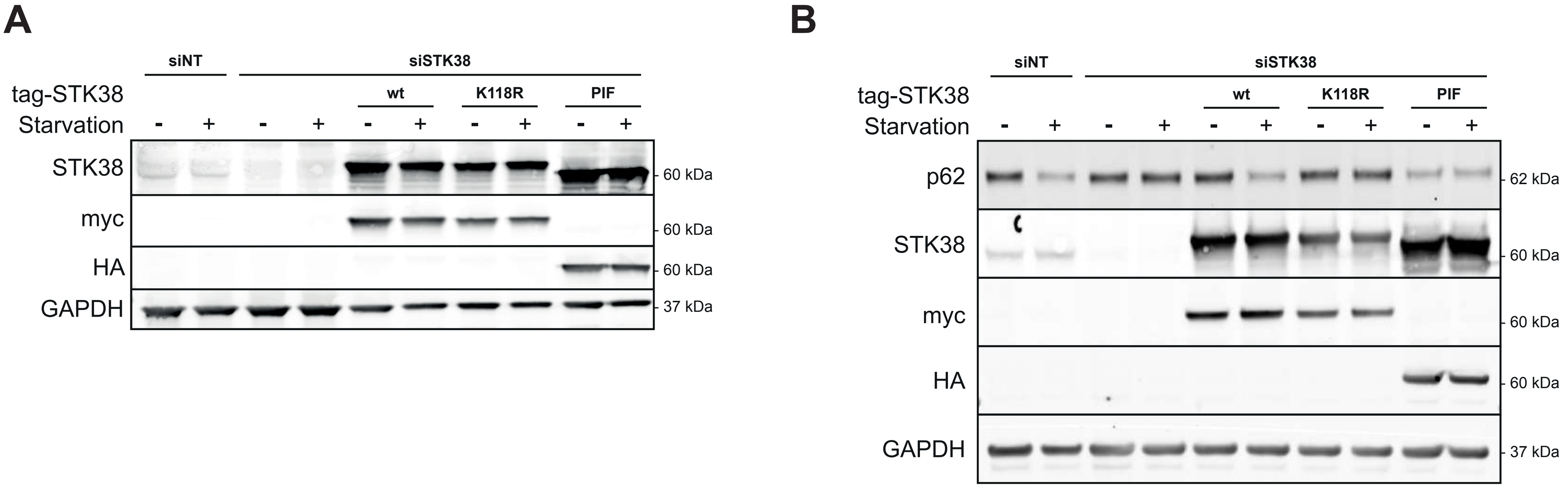

Martin et al. - Appendix Fig S4

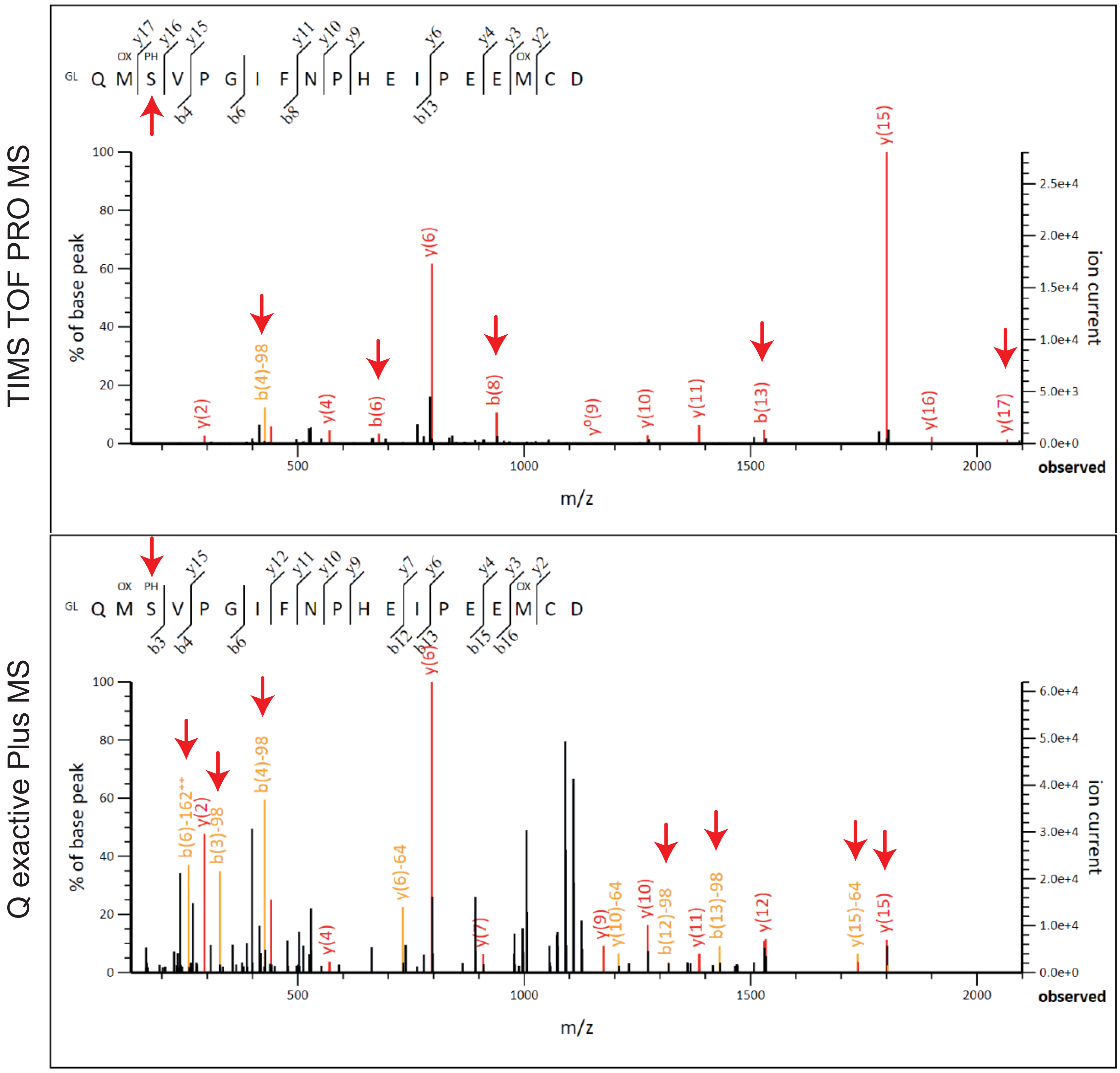

Martin et al. - Appendix Fig S5

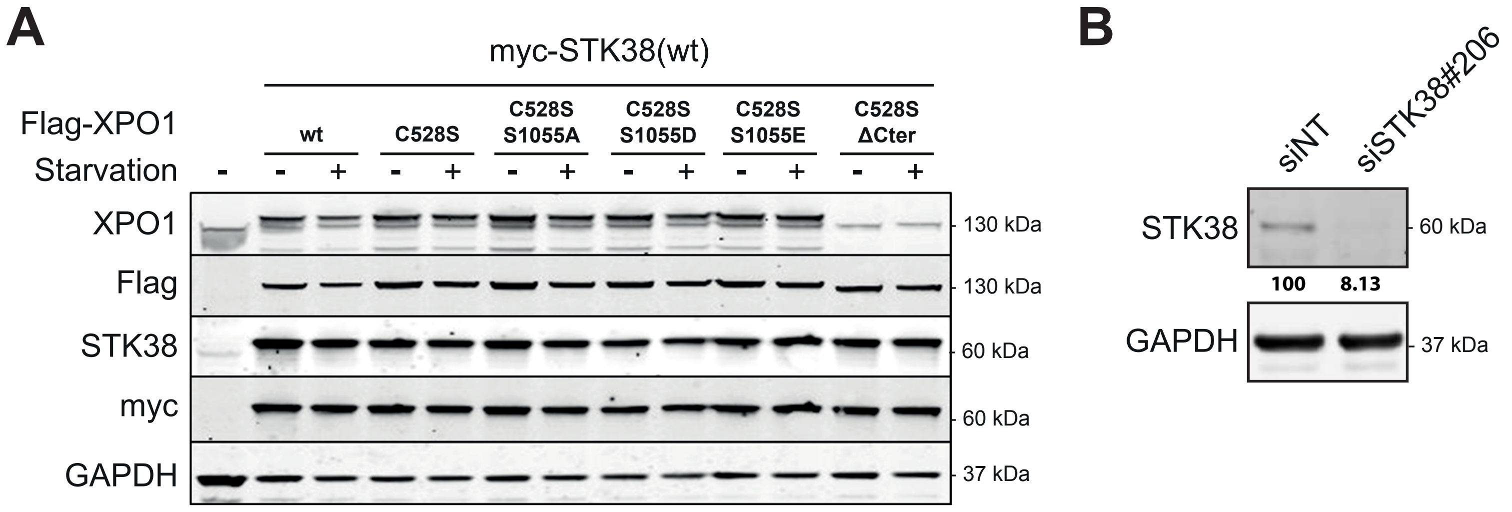

Martin et al. - Appendix Fig S6

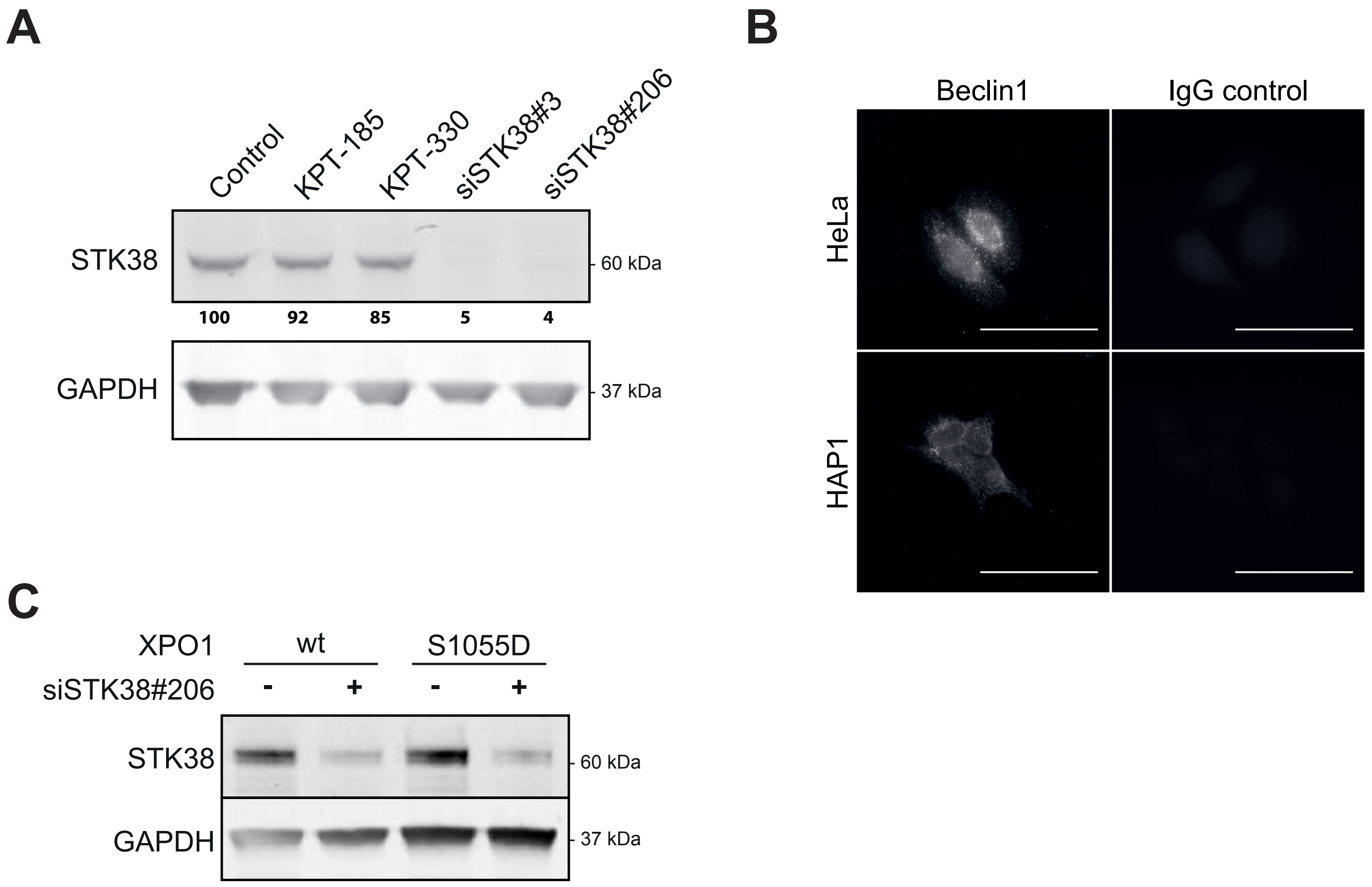

Martin et al. - Appendix Fig S7

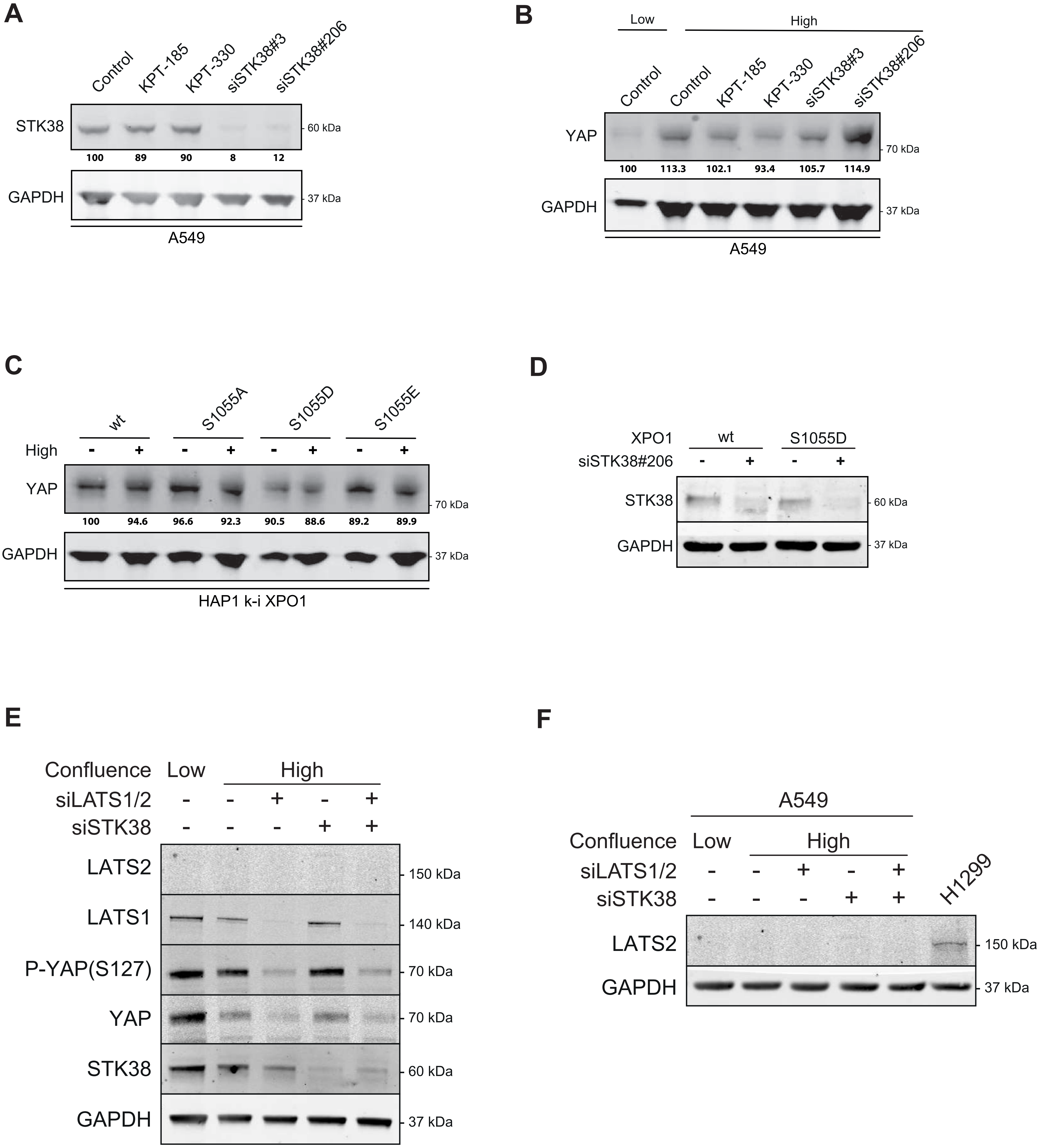

Martin et al. - Appendix Fig S8

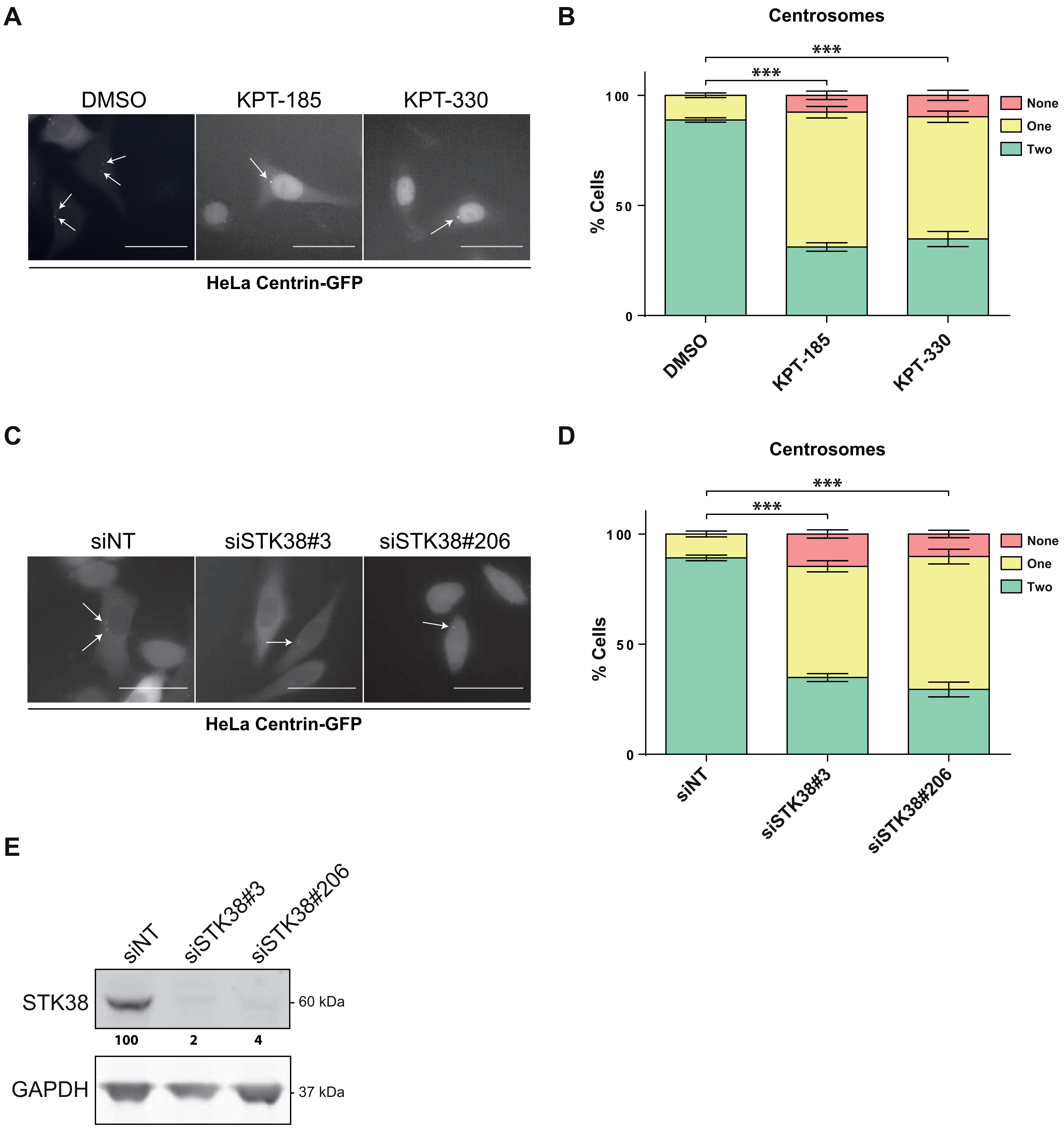

Martin et al. - Appendix Fig S9

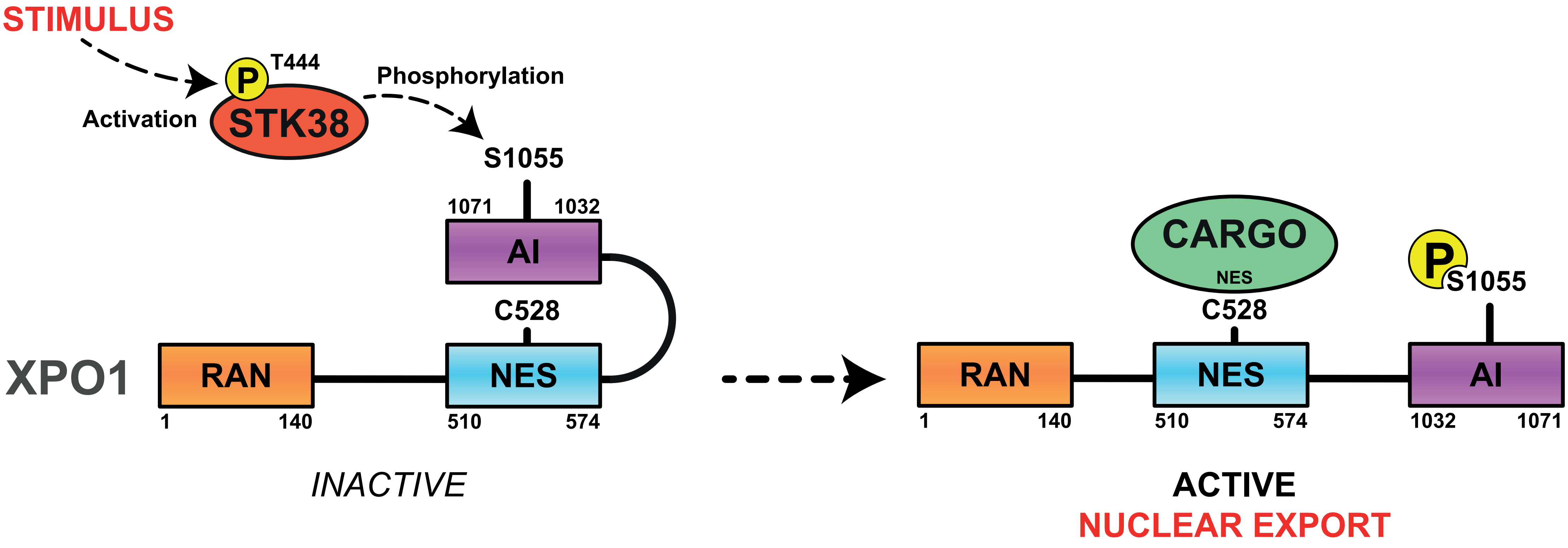

Martin et al. - Appendix Fig S10

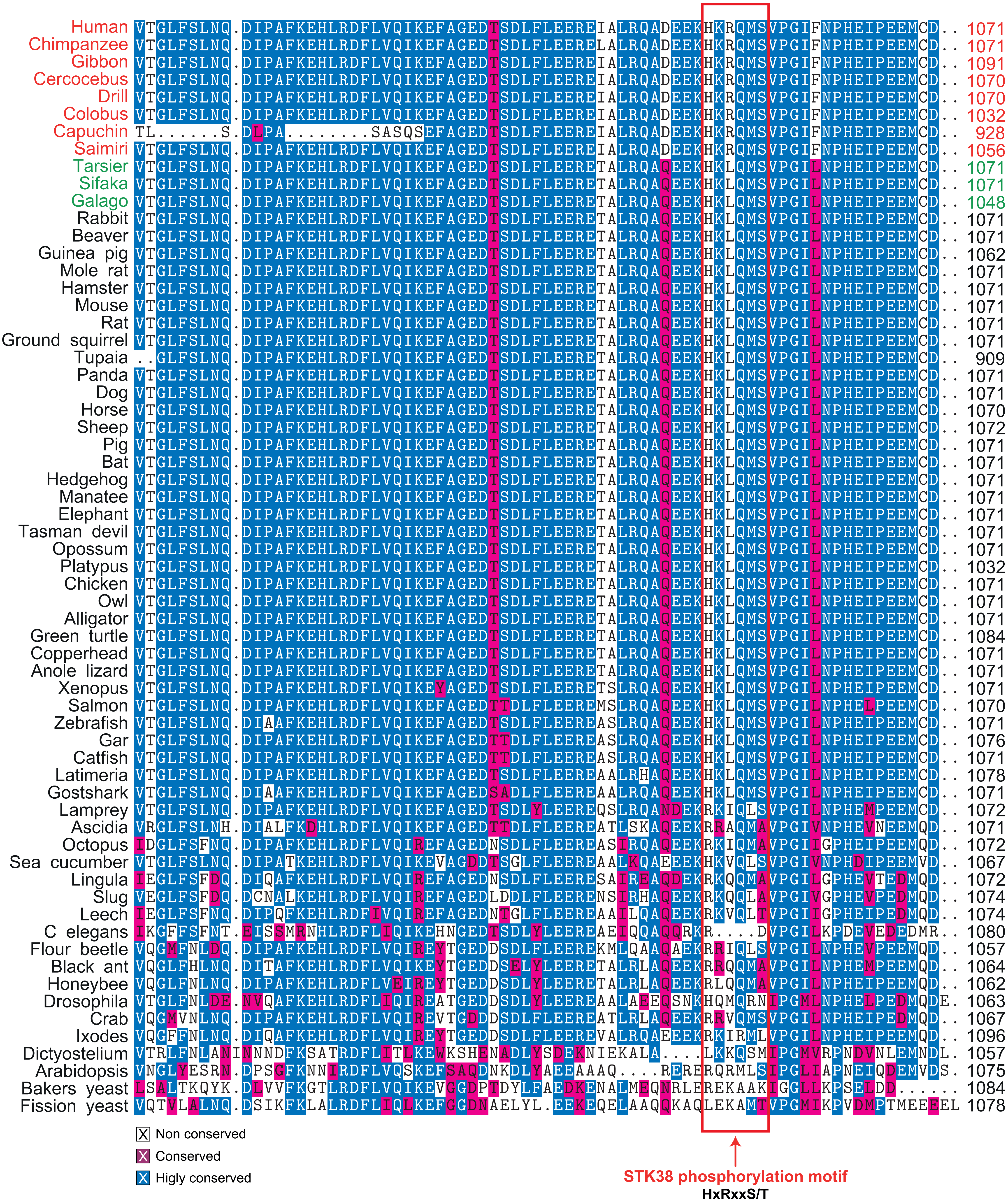

```
         Human VTGLFSLNQ.DIPAFKEHLRDFLVQIKEFAGEDTSDLFLEEREIALRQADEEKHKRQMSVPGIFNPHEIPEEMCD.. 1071
    Chimpanzee VTGLFSLNQ.DIPAFKEHLRDFLVQIKEFAGEDTSDLFLEERELALRQADEEKHKRQMSVPGIFNPHEIPEEMCD.. 1071
        Gibbon VTGLFSLNQ.DIPAFKEHLRDFLVQIKEFAGEDTSDLFLEEREIALRQADEEKHKRQMSVPGIFNPHEIPEEMCD.. 1091
    Cercocebus VTGLFSLNQ.DIPAFKEHLRDFLVQIKEFAGEDTSDLFLEEREIALRQADEEKHKRQMSVPGIFNPHEIPEEMCD.. 1070
         Drill VTGLFSLNQ.DIPAFKEHLRDFLVQIKEFAGEDTSDLFLEEREIALRQADEEKHKRQMSVPGIFNPHEIPEEMCD.. 1070
       Colobus VTGLFSLNQ.DIPAFKEHLRDFLVQIKEFAGEDTSDLFLEEREIALRQADEEKHKRQMSVPGIFNPHEIPEEMCD.. 1032
      Capuchin TL......S.DLPA........SASQSEFAGEDTSDLFLEEREIALRQADEEKHKRQMSVPGIFNPHEIPEEMCD.. 928
       Saimiri VTGLFSLNQ.DIPAFKEHLRDFLVQIKEFAGEDTSDLFLEEREIALRQADEEKHKRQMSVPGIFNPHEIPEEMCD.. 1056
       Tarsier VTGLFSLNQ.DIPAFKEHLRDFLVQIKEFAGEDTSDLFLEERETALRQAQEEKHKLQMSVPGILNPHEIPEEMCD.. 1071
        Sifaka VTGLFSLNQ.DIPAFKEHLRDFLVQIKEFAGEDTSDLFLEERETALRQAQEEKHKLQMSVPGILNPHEIPEEMCD.. 1071
        Galago VTGLFSLNQ.DIPAFKEHLRDFLVQIKEFAGEDTSDLFLEERETALRQAQEEKHKLQMSVPGILNPHEIPEEMCD.. 1048
        Rabbit VTGLFSLNQ.DIPAFKEHLRDFLVQIKEFAGEDTSDLFLEERETALRQAQEEKHKLQMSVPGILNPHEIPEEMCD.. 1071
        Beaver VTGLFSLNQ.DIPAFKEHLRDFLVQIKEFAGEDTSDLFLEERETALRQAQEEKHKLQMSVPGILNPHEIPEEMCD.. 1071
    Guinea pig VTGLFSLNQ.DIPAFKEHLRDFLVQIKEFAGEDTSDLFLEERETALRQAQEEKHKLQMSVPGILNPHEIPEEMCD.. 1062
      Mole rat VTGLFSLNQ.DIPAFKEHLRDFLVQIKEFAGEDTSDLFLEERETALRQAQEEKHKLQMSVPGILNPHEIPEEMCD.. 1071
       Hamster VTGLFSLNQ.DIPAFKEHLRDFLVQIKEFAGEDTSDLFLEERETALRQAQEEKHKLQMSVPGILNPHEIPEEMCD.. 1071
         Mouse VTGLFSLNQ.DIPAFKEHLRDFLVQIKEFAGEDTSDLFLEERETALRQAQEEKHKLQMSVPGILNPHEIPEEMCD.. 1071
           Rat VTGLFSLNQ.DIPAFKEHLRDFLVQIKEFAGEDTSDLFLEERETALRQAQEEKHKLQMSVPGILNPHEIPEEMCD.. 1071
Ground squirrel VTGLFSLNQ.DIPAFKEHLRDFLVQIKEFAGEDTSDLFLEERETALRQAQEEKHKLQMSVPGILNPHEIPEEMCD.. 1071
        Tupaia ..GLFSLNQ.DIPAFKEHLRDFLVQIKEFAGEDTSDLFLEERETALRQAQEEKHKLQMSVPGILNPHEIPEEMCD.. 909
         Panda VTGLFSLNQ.DIPAFKEHLRDFLVQIKEFAGEDTSDLFLEERETALRQAQEEKHKLQMSVPGILNPHEIPEEMCD.. 1071
           Dog VTGLFSLNQ.DIPAFKEHLRDFLVQIKEFAGEDTSDLFLEERETALRQAQEEKHKLQMSVPGILNPHEIPEEMCD.. 1071
         Horse VTGLFSLNQ.DIPAFKEHLRDFLVQIKEFAGEDTSDLFLEERETALRQAQEEKHKLQMSVPGILNPHEIPEEMCD.. 1070
         Sheep VTGLFSLNQ.DIPAFKEHLRDFLVQIKEFAGEDTSDLFLEERETALRQAQEEKHKLQMSVPGILNPHEIPEEMCD.. 1072
           Pig VTGLFSLNQ.DIPAFKEHLRDFLVQIKEFAGEDTSDLFLEERETALRQAQEEKHKLQMSVPGILNPHEIPEEMCD.. 1071
           Bat VTGLFSLNQ.DIPAFKEHLRDFLVQIKEFAGEDTSDLFLEERETALRQAQEEKHKLQMSVPGILNPHEIPEEMCD.. 1071
      Hedgehog VTGLFSLNQ.DIPAFKEHLRDFLVQIKEFAGEDTSDLFLEERETALRQAQEEKHKLQMSVPGILNPHEIPEEMCD.. 1071
       Manatee VTGLFSLNQ.DIPAFKEHLRDFLVQIKEFAGEDTSDLFLEERETALRQAQEEKHKLQMSVPGILNPHEIPEEMCD.. 1071
      Elephant VTGLFSLNQ.DIPAFKEHLRDFLVQIKEFAGEDTSDLFLEERETALRQAQEEKHKLQMSVPGILNPHEIPEEMCD.. 1071
  Tasman devil VTGLFSLNQ.DIPAFKEHLRDFLVQIKEFAGEDTSDLFLEERETALRQAQEEKHKLQMSVPGILNPHEIPEEMCD.. 1071
       Opossum VTGLFSLNQ.DIPAFKEHLRDFLVQIKEFAGEDTSDLFLEERETALRQAQEEKHKLQMSVPGILNPHEIPEEMCD.. 1071
      Platypus VTGLFSLNQ.DIPAFKEHLRDFLVQIKEFAGEDTSDLFLEERETALRQAQEEKHKLQMSVPGILNPHEIPEEMCD.. 1032
       Chicken VTGLFSLNQ.DIPAFKEHLRDFLVQIKEFAGEDTSDLFLEERETALRQAQEEKHKLQMSVPGILNPHEIPEEMCD.. 1071
           Owl VTGLFSLNQ.DIPAFKEHLRDFLVQIKEFAGEDTSDLFLEERETALRQAQEEKHKLQMSVPGILNPHEIPEEMCD.. 1071
     Alligator VTGLFSLNQ.DIPAFKEHLRDFLVQIKEFAGEDTSDLFLEERETALRQAQEEKHKLQMSVPGILNPHEIPEEMCD.. 1071
  Green turtle VTGLFSLNQ.DIPAFKEHLRDFLVQIKEFAGEDTSDLFLEERETALRQAQEEKHKLQMSVPGILNPHEIPEEMCD.. 1084
    Copperhead VTGLFSLNQ.DIPAFKEHLRDFLVQIKEFAGEDTSDLFLEERETALRQAQEEKHKLQMSVPGILNPHEIPEEMCD.. 1071
   Anole lizard VTGLFSLNQ.DIPAFKEHLRDFLVQIKEFAGEDTSDLFLEERETALRQAQEEKHKLQMSVPGILNPHEIPEEMCD.. 1071
       Xenopus VTGLFSLNQ.DIPAFKEHLRDFLVQIKEYAGEDTSDLFLEERETSLRQAQEEKHKLQMSVPGILNPHEIPEEMCD.. 1071
        Salmon VTGLFSLNQ.DIPAFKEHLRDFLVQIKEFAGEDTTDLFLEEREMSLRQAQEEKHKLQMSVPGILNPHELPEEMCD.. 1070
     Zebrafish VTGLFSLNQ.DIAAFKEHLRDFLVQIKEFAGEDTSDLFLEEREASLRQAQEEKHKLQMSVPGILNPHEIPEEMCD.. 1071
           Gar VTGLFSLNQ.DIPAFKEHLRDFLVQIKEFAGEDTTDLFLEEREASLRQAQEEKHKLQMSVPGILNPHEIPEEMCD.. 1076
       Catfish VTGLFSLNQ.DIPAFKEHLRDFLVQIKEFAGEDTTDLFLEEREASLRQAQEEKHKLQMSVPGILNPHEIPEEMCD.. 1071
     Latimeria VTGLFSLNQ.DIPAFKEHLRDFLVQIKEFAGEDTSDLFLEEREAALRHAQEEKHKLQMSVPGILNPHEIPEEMCD.. 1078
     Gostshark VTGLFSLNQ.DIAAFKEHLRDFLVQIKEFAGEDSADLFLEEREAALRQAQEEKHKLQMSVPGILNPHEIPEEMCD.. 1071
       Lamprey VTGLFSLNQ.DIPAFKEHLRDFLVQIKEFAGEDTSDLYLEEREQSLRQANDEKRKIQLSVPGILNPHEMPEEMCD.. 1072
      Ascidia VRGLFSLNH.DIALFKDHLRDFLVQIKEFAGEDTTDLFLEEREATLSKAQEEKRRAQMAVPGIVNPHEVNEEMQD.. 1071
       Octopus IDGLFSFNQ.DIPAFKEHLRDFLVQIREFAGEDNSDLFLEEREASIRQAQEEKRKIQMAVPGIIGPHEIPEEMQD.. 1072
  Sea cucumber VTGLFSLNQ.DIPATKEHLRDFLVQIKEVAGDDTSGLFLEEREAALKQAEEEKHKVQLSVPGIVNPHDIPEEMVD.. 1067
       Lingula IEGLFSFDQ.DIQAFKEHLRDFLVQIREFAGEDNSDLFLEERESAIREAQDEKRKQQMAVPGILGPHEVTEDMQD.. 1072
          Slug VEGLFSFDQ.DCNALKEHLRDFLVQIREFAGEDLDDLFLEERENSIRHAQEEKRKQQLAVPGIVGPHEVPEDMQD.. 1074
         Leech IEGLFSFNQ.DIPQFKEHLRDFIVQIREFAGEDNTGLFLEEREAAILQAQEEKRKVQLTVPGIIGPHEIPEDMQD.. 1074
     C elegans IKGFFSFNT.EISSMRNHLRDFLIQIKEHNGEDTSDLYLEEREAEIQQAQQRKR....DVPGILKPDEVEDEDMR.. 1080
  Flour beetle VQGMFNLDQ.DIPAFKEHLRDFLVQIREYTGEDDSDLFLEEREKMLQAAQAEKRRIQLSVPGILNPHEVPEEMQD.. 1057
     Black ant VQGLFHLNQ.DITAFKEHLRDFLVQIKEYTGEDDSELYLEERETALRLAQEEKRRQQMAVPGILNPHEMPEEMQD.. 1064
      Honeybee VQGLFNLNQ.DIPAFKEHLRDFLVEIREYTGEDDSDLYLEERETALRLAQEEKRLQQMAVPGILNPHEIPEEMQD.. 1062
    Drosophila VTGLFNLDE.NVQAFKEHLRDFLIQIREATGEDDSDLYLEEREAALAEEQSNKHQMQRNIPGMLNPHELPEDMQDE. 1063
          Crab VQGMVNLNQ.DIPAFKEHLRDFLVQIREVTGDDDSDLFLEEREATLRLAQEEKRRVQMSVPGILNPHEIPEDMQD.. 1067
        Ixodes VQGFFNLNQ.DIQAFKEHLRDFLVQIREYTGEDDSDLFLEEREVALRQAEEEKRKIRMLVPGILNPHEIPEEMQD.. 1096
 Dictyostelium VTRLFNLANINNNDFKSATRDFLITLKEWKSHENADLYSDEKNIEKALA....LKKQSMIPGMVRPNDVNLEMNDL. 1057
   Arabidopsis VNGLYESRN.DPSGFKNNIRDFLVQSKEFSAQDNKDLYAEEAAAQ....RERERQRMLSIPGLIAPNEIQDEMVDS. 1075
  Bakers yeast LSALTKQYK.DLVVFKGTLRDFLVQIKEVGGDPTDYLFAEDKENALMEQNRLEREKAAKIGGLLKPSELDD...... 1084
 Fission yeast VQTVLALNQ.DSIKFKLALRDFLIQLKEFGGDNAELYL.EEKEQELAAQQKAQLEKAMTVPGMIKPVDMPTMEEEEL 1078
```

☐ Non conserved

▨ Conserved

🟦 Higly conserved

STK38 phosphorylation motif

HxRxxS/T